

Nuclear Magnetic Resonance and Quadrupole Interactions in Some Dilute Aluminum Alloys*

L. E. Drain†

Materials Science Division, Argonne National Laboratory, Argonne, Illinois 60439

(Received 26 February 1973)

Studies have been made of the ^{27}Al magnetic resonance from dilute alloys of aluminum with silver, gallium, germanium, magnesium, and copper using powder and foil samples. The satellite structure observed is interpreted in terms of quadrupole interaction at sites that neighbor the solute atoms. The values of the quadrupole interaction parameter ν_Q at the aluminum-nearest-neighbor silver, gallium, germanium, magnesium, and copper atoms were found to be 170 ± 3 , 174 ± 1 , 250 ± 1 , 155 ± 2 , and 121 ± 2 kHz, respectively. The corresponding asymmetry factors are 0.31 ± 0.02 , 0.017 ± 0.017 , 0.053 ± 0.001 , 0.05 ± 0.01 , and 0.06 ± 0.02 . To obtain sufficient sensitivity, most measurements were made at 4.2°K. However, in the gallium and germanium alloys, measurements were also possible at room temperature where the quadrupole interaction was found to be reduced by about 6%. In the gallium and magnesium alloys, further structure was observed and was attributed to the second-neighbor positions. Gallium and copper nuclear magnetic resonances were observed in the appropriate alloys. The Knight shifts were $(0.490 \pm 0.005)\%$ and $(0.35 \pm 0.01)\%$, respectively. The ^{69}Ga and ^{63}Cu resonances are closely Gaussian in shape, but the linewidth was greater than could be attributed to nuclear dipolar interactions only. Measurements of intensity showed that the signals observed were essentially from the central ($m = -1/2$ to $m = 1/2$) transition only. To assist in the interpretation of the quadrupole structure from polycrystalline samples, formulas were derived for the theoretical intensities of the satellite peaks. An analysis was also made of the line shapes that arise from quadrupole interactions having a small but nonzero asymmetry factor.

I. INTRODUCTION

The effect of quadrupole interactions on nuclear magnetic resonance (NMR) in dilute alloys is well known. Early studies of copper¹ and aluminum² alloys showed that the intensity of resonance from a powdered sample decreases rapidly as the concentration of the solute increases. This could be quantified in terms of a parameter N , the effective number of nuclei that neighbor a solute atom whose resonance is lost because of broadening by quadrupole effects. The long range of these quadrupole interactions, deduced from the large values of N that are observed (about 100–200 for aluminum alloys), has been interpreted in terms of the long-range oscillations in electron density which theory predicts are around impurity atoms in a metal.^{3,4} More detailed information about these quadrupole interactions is thus of considerable interest.

Associated with each neighbor position around an impurity atom is a specific nuclear quadrupole interaction that is expected to be dependent on the type of impurity atom and the distance from this atom. It has been found possible to determine the values of some of these interactions experimentally in a few systems. Results for neighbors of silver, gallium, germanium, copper, and magnesium atoms in solution in aluminum are reported in this paper.

Nuclear quadrupole interactions are obtained from the splitting of NMR spectra. In principle, this can be most readily studied in single-crystal

samples, and measurements on single crystals of some copper and aluminum alloys have recently been reported.^{5,6} However, good signals are not easy to obtain from metallic samples owing to the poor penetration of the radio-frequency (rf) field into the metal crystals due to the skin effect.

The experiments reported in the present paper were made on randomly oriented polycrystalline powder or foil samples. These are comparatively easy to prepare, and virtually complete penetration of the sample by the rf field may be achieved. The principal disadvantage is that the quadrupole structure of the resonance is largely smeared out by the random orientation of the crystallites. However, information about the quadrupole interactions can be obtained from residual peaks in the tails of the nuclear resonance curves. The peaks are due to singularities in the distribution function of resonance frequencies or "powder pattern." As in most methods of studying impurity effects, it is necessary to restrict the concentration to avoid the complication of overlapping regions of influence of the impurity atoms. The atomic concentration should evidently be rather less than $1/N$, i. e., less than about 1 at. % for most of the aluminum alloys. The fraction of nuclei that have a specific quadrupole interaction is thus rather small, and the resultant peaks in the derivative NMR spectra are expected to have only 10^{-3} to 10^{-5} of the amplitude of the main ^{27}Al resonance. To achieve the high sensitivity required, the use of low temperatures and/or signal-averaging techniques is usually necessary.

The spin of the nucleus of ^{27}Al is $\frac{5}{2}$. Thus the magnetic resonance is split by quadrupole interaction into five components that are, in first-order approximation, equally spaced, in which the central line is unshifted from the unperturbed position. Except in one case, the first-order approximation is adequate for the analysis of the experiments described here. We thus expect observable features of the line shape due to quadrupole splitting to be associated in sets of four, corresponding to the four satellite lines. It is convenient to distinguish the satellites by a number n , which denotes transitions between the $(n - \frac{1}{2})$ and $(n + \frac{1}{2})$ magnetic quantum levels. Thus the inner pair of satellites is denoted by $n = \pm 1$ and the outer pair by $n = \pm 2$.

The quadrupole interaction at a site that neighbors an impurity atom may or may not have axial symmetry depending on the crystal symmetry at the site. In the face-centered-cubic (fcc) structure of aluminum, the first neighbor of a substitutional impurity is at a position with only a twofold rotational axis of symmetry. Thus the quadrupole interaction associated with this nucleus is, in general, asymmetric although in most cases the degree of asymmetry is not large. At the second-neighbor position, however, the rotation axis is fourfold which automatically ensures an axially symmetric quadrupole interaction.

The relation of the satellite peaks in the magnetic resonance to these quadrupole interactions is discussed in the Appendix. In principle, the change in Knight shift at a neighbor position may also be determined, as this results in a shift of the relevant pattern of satellite peaks with respect to the main resonance. In aluminum alloys, however, no evidence for this effect has been found.

II. EXPERIMENTAL METHOD

The NMR measurements were made with a Varian wide-line spectrometer. The 9-in. electromagnet, stabilized with a "field-dial" Hall probe, was run at about 14 kG. To obtain adequate rf stability during the long times often necessary for experiments, the rf oscillator of the spectrometer was normally locked to a crystal oscillator that generated 15.5 MHz, the usual frequency of measurement. A specially designed crossed-coil probe described elsewhere,⁷ that could be cooled with the sample to liquid-helium temperatures, was used. This system eliminates the need for thermal insulation between the probe and sample, and thus gives a high filling factor and permits an efficient helium Dewar to be used. Runs lasting more than 2 days could be made with one filling of liquid helium. To avoid possible microphonic problems with the bubbling liquid, the space inside the can that contains the probe and sample was filled with gaseous helium kept at a

pressure somewhat below that of the liquid bath (usually atmospheric).

The normal audio-frequency (af) modulation and lock-in detection system was used, and 40 Hz was found to be the most satisfactory frequency. The modulation amplitude was usually 5.4 G (peak to peak), but was increased to 8.6 G for maximum sensitivity or was decreased to 2.7 G if an accurate line-shape measurement was required. Output time constants up to 60 sec were used with sweep times up to 4 h. For some of the work, a Northern Scientific signal averager was available. This was generally run overnight accumulating sweeps, each of 5-min duration using a 4-sec time constant.

Normally the rf balance was set for a signal of the pure-absorption mode. This critical adjustment was made by trial and error using the symmetry of the main ^{27}Al resonance, particularly in the outer regions of the curve, as a guide. Sometimes a small admixture of dispersion phase could be helpful in resolving some quadrupole structures close to the main peak.

Alloys of aluminum with 0.5-at.% Ga, 0.5-at.% Ag, and 0.2-at.% Cu were made by levitation melting in an rf induction heater under an argon atmosphere. To minimize the loss of solute metal, the small pieces required were inserted into holes drilled in 5-g pieces of zone-refined aluminum before melting. The alloy ingots were homogenized by annealing for about 1 day at 620 °C. Ingots of Al-Ag and Al-Ga were subdivided by filing. The powder was sieved through 325 mesh ($\sim 50 \mu\text{m}$) and, to remove the undesirable effect of cold work, annealed (under argon) overnight at 380 °C. This temperature was not sufficiently high to allow any sintering of the powder. Powder samples, of similar particle size, of the alloys Al-0.5-at.% Ge and Al-0.4-at.% Mg were kindly lent by T.J. Rowland⁸ and M. Minier,⁹ respectively. About 1 g of powder was required to fill the sample tube. Except for the gallium alloy, the particle size appeared to be sufficiently small because no appreciable loss of signal from the skin effect was observed even at liquid-helium temperature. (This is not true for pure aluminum.)

Two foil samples were made of the alloys Al-0.2-at.% Cu and Al-0.5-at.% Ga. The annealed ingots were rolled to a thickness of $\sim 15 \mu\text{m}$ (0.0006 in.), cut into pieces approximately $8 \times 15 \text{ mm}$, and stacked alternately with insulating "Kapton" film $6 \mu\text{m}$ (0.00025 in.) thick. About 200 layers were required to fill the sample volume. Foil samples were not quite as satisfactory as powder samples for, although a somewhat higher filling factor could be achieved, the samples were more prone to increase the electronic noise level, presumably from microphonic effects.

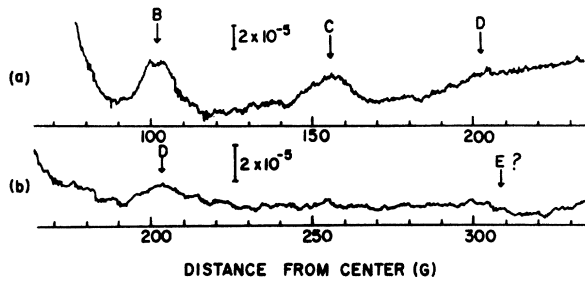


FIG. 1. ^{27}Al magnetic resonance curves from the Al-0.5-at.%-Ag alloy at 4.2°K that show quadrupole satellite peaks. The scale of the signal amplitude relative to the peak-to-peak amplitude of the main resonance is indicated. The signals were averaged over (a) 204 and (b) 279 5-min sweeps.

III. RESULTS

A. Aluminum-Silver

The quadrupole structure of this alloy was the most difficult to observe, and measurements were attempted to 4.2°K only. Three peaks (on either side of resonance), *B*, *C*, and *D* in Fig. 1, were definitely seen. Their positions and amplitudes relative to the central resonance are listed in Table I. There was some doubt about the existence of peak *A*. Unusually long-“tail” spreading out from the central resonance prevented the consistent resolution of this close-in peak.

The low intensity of the peaks suggests that they arise from an asymmetric quadrupole interaction and, if this is assumed, all peaks can be explained by a single interaction. We note that peak *C* must be an inner ($n = \pm 1$) satellite, since otherwise a peak at 78 G from the center would have been observed. The similar amplitude of peaks *B* and *C* suggests that *B* is from an inner satellite also, which is confirmed by the presence of the corresponding outer satellite *D*. We can now assign the

peaks to singularities in the quadrupole powder pattern.

It is indicated in the Appendix that, for the satellites $\pm n$, the singularities occur at frequency separations from the center of resonance of $\pm n\nu_Q$, $\pm \frac{1}{2}n(1 - \frac{1}{2}\eta)\nu_Q$, and $\pm \frac{1}{2}n(1 + \frac{1}{2}\eta)\nu_Q$, where η is the asymmetry factor. The quadrupole parameter is related to the quadrupole coupling constant by Eq. (2) of the Appendix. The separations in terms of the magnetic field are, of course, given by multiplying by $2\pi/\gamma$, where γ is the nuclear magnetogyric ratio. It thus follows that if we interpret *B* and *C* as arising from inner satellites, another inner satellite peak must be at a separation of either about 57 or 250 G. Clearly, only the first alternative is in accord with experiment, and it appears that peak *A* is genuine. The corresponding outer satellite peak expected at approximately 110 G is presumably unresolved from peak *B*.

The interpretation of the pattern derived leads to the following values for the quadrupole parameters: $\nu_Q = 170 \pm 3$ kHz and $\eta = 0.31 \pm 0.02$. Because of the magnitude of this interaction and the rather large asymmetry factor, it must be attributed to the first-neighbor position. To verify this, these values may be used to calculate the expected positions and amplitudes of the peaks using the theory given in the Appendix. (The wipeout number has been taken to be¹⁰ 205 and the dipolar broadening parameter $\sigma = 4.7$ kHz.¹¹) The results are listed in Table I. Although it is satisfactory that the relative values of the experimental amplitudes of the various satellite peaks agree quite well with calculation, all the amplitudes measured are less than their calculated values by a factor of about 4. The probable explanation is that the amount of silver actually in solid solution is much smaller than the nominal composition would indicate. Obtaining an adequate concentration of silver in solid solution is difficult. Any precipitation, clustering, or pairing of atoms reduces the number of nuclei that have exactly the

TABLE I. Satellite peaks from the Al-0.5-at.%-Ag alloy. Theoretical values were calculated with the parameters $\nu_Q = 170$ kHz, $\eta = 0.31$, $N = 205$, and $\sigma = 4.7$ kHz. All peaks are from the first-neighbor position.

Peak	Separation from center of resonance (G)	Amplitude relative to main resonance ($\times 10^{-5}$)	Type of singularity ^a	Satellite no. <i>n</i>	Theoretical separation (G)	Theoretical relative amplitude ($\times 10^{-5}$)
<i>A</i>	60 ± 3	5 ± 5	<i>L</i>	1	59	14.7
<i>B</i>	101 ± 2	5 ± 1	<i>S</i>	1	100	14.5
...	Not resolved		<i>L</i>	2	111	4.6
<i>C</i>	153 ± 3	2.7 ± 0.5	<i>S</i>	1	153	7.3
<i>D</i>	202 ± 4	0.9 ± 0.3	<i>S</i>	2	201	4.5
<i>E</i>	...	< 0.4	<i>S</i>	2	306	2.3

^a*L* is logarithmic infinity and *S* is step singularity.

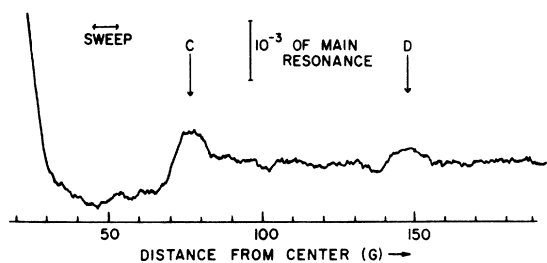


FIG. 2. Quadrupole structure of the ^{27}Al resonance from the Al-0.5-at.-%-Ga alloy (powder sample) observed at room temperature at 15.5 MHz. The sweep time was 100 min, and the time constant was 1 min.

same quadrupole interaction and hence the amplitude of the quadrupole structure observed.

B. Aluminum-Gallium

By contrast with Al-Ag, quadrupole structure in the Al-0.5-at.-%-Ga alloy was readily observed even at room temperature (Fig. 2). The two strong peaks observed on either side of resonance (called C and D in Table II) are clearly the inner and outer satellites of an axially symmetric (or nearly so) quadrupole interaction with $\nu_Q = 166$ kHz (at 300 °K). Measurements at 77 °K showed two additional peaks (A and B) closer to the main resonance with spacings from the center in the ratio of 1:2 (Fig. 3). The peaks are evidently related to another smaller quadrupole interaction.

Reducing the temperature of the powder sample to 4.2 °K did not give the greatly improved signal obtained with the other alloys. Also an unusual setting of the rf bridge was required to produce an absorption signal. These phenomena indicate the presence of a pronounced skin effect, but this is surprising since the published value of the residual resistivity for gallium in aluminum¹² is not very

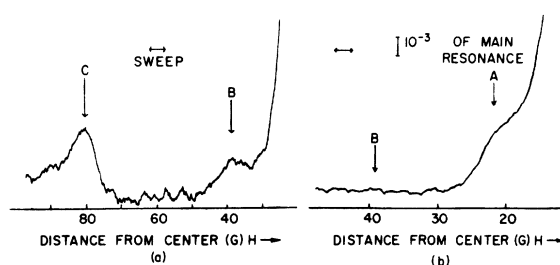


FIG. 3. ^{27}Al resonance curves from the Al-0.5-at.-%-Ga alloy at 77 °K, that show the peaks (A and B) close to the main resonance attributed to the quadrupole interaction at the second-neighbor position.

different from that for other impurities, e.g., zinc (see Table III). As would be expected, the foil sample produced better results at liquid-helium temperatures since the foil thickness was about three times less than the diameter of the particles of the powder sample. Overnight averaging with this sample enabled the observation of the further peak E. This is the outer step singularity from the quadrupole interaction associated with peaks C and D.

The positions of all peaks are listed in Table II. These results are in substantial agreement with those of Berthier and Minier.¹³ No significant differences between the powder and foil samples were observed, but the results of intensity measurements on the foil sample were not taken into account. Because of possible preferred orientation produced by rolling, these results may not be representative of the random crystallite orientation assumed in the theory.

The main problem in the interpretation of these results is whether to assign the largest ($\nu_Q = 174$ kHz) interaction to the first- or second-neighbor position. The magnitude of the interaction suggests

TABLE II. Satellite peaks from the Al-0.5-at.-%-Ga alloys. Theoretical values were calculated with the parameters $N=160$ and $\sigma=4.7$ kHz: $\nu_Q=174$ kHz and $\eta=0$ for first neighbor position and $\nu_Q=41$ kHz and $\eta=0$ for second neighbor position.

Peak	Separation from center of resonance (G)	Amplitude relative to main resonance ($\times 10^{-5}$)	Type of singularity ^a	Satellite no. n	Theoretical separation (G)	Theoretical relative amplitude ($\times 10^{-5}$)
A ^b	21 ± 1	100 ± 30	R	1	21	116
B ^b	39 ± 1	30 ± 10	{R S}	{2 1}	39	{51 16} 61
...	Not resolved		S	2	74	5
C ^c	80 ± 1	100 ± 5	R	1	80.6	113
D ^c	159 ± 1	32 ± 3	{R S}	{2 1}	159	{50 8} 55
E ^c	319 ± 4	...	S	2	313	2

^aR is inverse square-root infinity and S is step singularity.

^cMeasured at 4.2 °K.

^bMeasured at 77 °K.

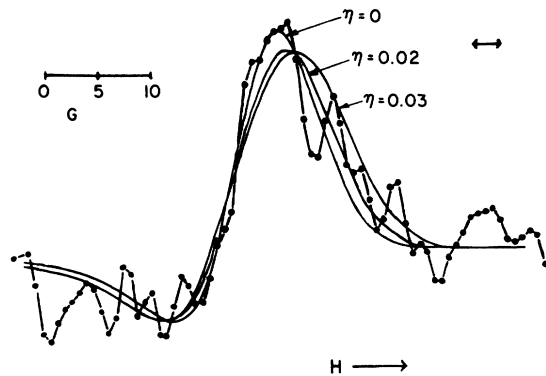


FIG. 4. Line shape of the inner satellite (peak C) of the 174 kHz quadrupole interaction in the Al-0.5-at.-%-Ga alloy. The experimental curve obtained by signal averaging 256 5-min sweeps at 77°K is compared with calculated line shapes based on different values of η .

that it arises from first neighbors. However, the absence of any evidence of deviation from axial symmetry indicates a position that has automatic axial symmetry, presumably the second-neighbor site. Careful measurements of the amplitudes of peaks C and D were used to decide this question. If the interaction is assumed to be from the second neighbors, the amplitudes relative to the main resonance calculated from formula (12) of the Appendix (using $N=160^{10}$ and $\sigma=4.7$ kHz) are 5.8×10^{-4} and 2.5×10^{-4} for peaks C and D, respectively. Since the experimental values are greater than these beyond experimental error, this assumption cannot be correct. Although a decrease in experimental intensity can be explained in a number of ways, e.g., loss of solute during melting or precipitation, an increase in intensity cannot be explained except by assuming that more neighbor sites are involved. It is thus concluded that the 174-kHz interaction must be assigned to the nearest-neighbor

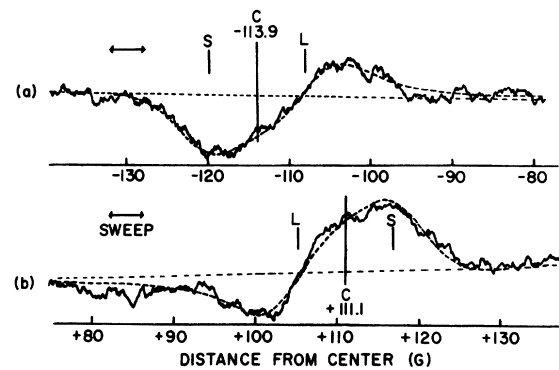


FIG. 5. Traces of the inner satellite peaks of the ^{27}Al resonance from the Al-0.5-at.-%-Ge alloy at 4.2°K. The theoretical line shape for $\eta=0.053$ (dashed curves) agrees closely with experiment. The positions of the logarithmic (L) and step (S) singularities of the unbroadened powder pattern are indicated.

bor positions with 12 per solute atom rather than the next-neighbor positions with only 6. This interpretation leads to a more reasonable relation of experimental and theoretical amplitudes. The values are compared in Table II.

It is surprising that the asymmetry factor for the nearest-neighbor position is so close to zero, especially for this alloy where the solute and solvent have equal valence but appreciable size difference. An effort was made to detect a slight deviation from zero by a careful study of the line shape of peak C. An averaged curve using a small modulation amplitude is shown in Fig. 4. Best-fitting theoretical curves, assuming different values of η , are shown superimposed on the experimental curve. The calculation of the line shape for this almost axially symmetric situation is described in the Appendix. It will be seen that the best fit between theory and experiment is with $\eta=0.02$, but 0 and 0.03 are not excluded. The curve for $\eta=0.035$ (not shown in

TABLE III. Properties of dilute aluminum alloys with various solutes.

Solute	Quadrupole interactions			^{27}Al wipe-out number	Valency difference	Lattice distortion coefficient (1/a) (da/dc)	Residual resistivity ($\mu\Omega$ -cm/at.%)
	First neighbor ν_Q (kHz)	η	Second neighbor ν_Q (kHz)				
Mg	155 ± 2	0.05 ± 0.01	49 ± 1	130 ^a	-1	+0.11 ^b	0.44 ^c
Cu	121 ± 2	0.06 ± 0.02	< 70	236 ^d	-2	-0.12 ^b	0.8 ^c
Zn	138 ± 2	0.25 ± 0.01	25 ± 1	98 ^a	-1	-0.023 ^b	0.24 ^c
Ga	174 ± 1	0.017 ± 0.017	41 ± 2	160 ^d	0	+0.05 ^b	0.24 ^e
Ge	250 ± 1	0.053 ± 0.001	< 40	120 ^f	+1	+0.04 ^b	0.78 ^c
Ag	170 ± 3	0.31 ± 0.02	< 80	205 ^d	-2	+0.023 ^g	1.1 ^c

^aReference 2.

^bReference 23.

^cA. T. Robinson and J. E. Dorn, Trans AIME (J. Metals) 191, 457 (1951).

^dReference 10.

^eReference 12.

^fT. J. Rowland (private communication).

^gCalculated by Fukai (Ref. 22) from the results of Beaman, Balluffi, and Simons, [Phys. Rev. 134, A532 (1964)].

Fig. 4) was clearly too wide. We thus deduce $\eta = 0.017 \pm 0.017$. In the calculation, a Gaussian broadening function, peak-to-peak width of 8.4 G $\sigma = 4.7$ kHz was assumed. This value was obtained from earlier measurements on Al-Zn alloys.¹¹ However, a considerable variation is allowable without affecting the value of η deduced.

We now consider the interpretation of the two close-in peaks *A* and *B* (Fig. 3). The calculated amplitude ratios given in Table II assume that the peaks arise from the second neighbors with $\nu_Q = 41$ kHz, and this appears to be the correct interpretation. An alternative explanation is in terms of a 20-kHz interaction, but if this were associated with second neighbors, the calculated amplitude ratios for peaks *A* and *B* would be 93×10^{-5} and 10×10^{-5} , clearly incorrect. However, we cannot completely exclude the possibility that this interaction is associated with the 24 third-neighbor positions or the 12 fourth-neighbor positions as suggested by Berthier and Minier.¹³

C. Aluminum-Germanium

Only two satellite peaks (on each side of resonance) were observed in the Al-Ge alloy. The mean separations from the center of resonance were 117 and 235 G, respectively (at 4.2 °K). The peaks were clearly broadened and unusually shaped, which indicates incipient resolution of separate peaks from nonaxial symmetry. As shown in Fig. 5, line shapes calculated by the method given in the Appendix fitted the experimental curves well, and we thus deduce $\nu_Q = 250$ kHz and $\eta = 0.053 \pm 0.001$. It will be seen from Fig. 5 that the peaks are not exactly symmetrically placed about the resonance center. The shift of the peaks is -1.4 ± 0.4 G. The calculated second-order quadrupole shift for these inner satellite peaks is -1.13 G. Thus this provides a satisfactory explanation, and we conclude that there is no evidence of any change in Knight shift at the first-neighbor position of more than 0.003%.

The theoretical amplitudes of the satellite peaks (relative to the main resonance) were calculated using the theory given in the Appendix. The values obtained, 60×10^{-5} and 17×10^{-5} for the inner and outer satellites, respectively, agree well with the measured values of $(53 \pm 5) \times 10^{-5}$ and $(12 \pm 3) \times 10^{-5}$.

A search for other satellite peaks showed that

TABLE IV. Temperature dependence of the nuclear quadrupole interaction at first neighbors of solute atoms in aluminum.

Solute	Quadrupole interaction parameter ν_Q (kHz)		
	4.2 °K	77 °K	300 °K
Ga	174 ± 1	174 ± 1	166 ± 1
Ge	250 ± 1	250 ± 3	233 ± 4

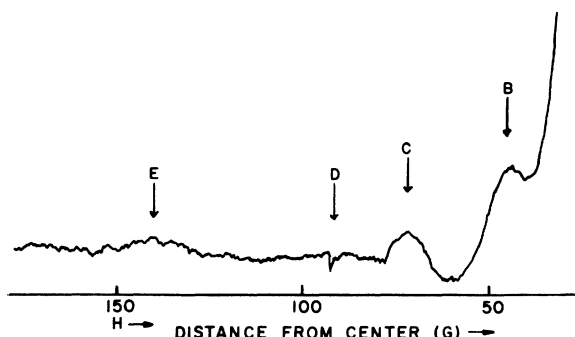


FIG. 6. Quadrupole structure of the ^{27}Al resonance from the Al-0.4-at.-%-Mg alloy, a 2-hr trace at 4.2 °K with a time constant of 1 min.

there were none of relative amplitude greater than 50×10^{-5} beyond 37 G from the center. We can thus set an upper limit of $\nu_Q = 40$ kHz to the quadrupole interaction at the second-neighbor site.

As discussed for the gallium alloy, it was possible to observe quadrupole structure in the germanium alloy at 77 and 300 °K. Experimental values of the quadrupole parameters at 4.2, 77, and 300 °K are listed in Table IV for these two alloys. A significant temperature dependence is observed. Unfortunately, the signals at the higher temperatures were not good enough to allow η to be determined.

D. Aluminum-Magnesium

In this alloy, five quadrupole satellite peaks (on either side of resonance) were definitely observed. Except for the innermost peak, these appear in the trace shown in Fig. 6. A further peak (*F*) nearly 300 G from the center was almost certainly present. The peaks and their observed amplitudes relative to the main resonance are listed in Table V. Peak *E* has also been seen by Fernelius and Slichter.¹⁴

Two quadrupole interactions are involved, 155 and 49 kHz, each with approximately $\eta = 0$. It is natural to assign the larger interaction to the first-neighbor position and the smaller to the second neighbor. However, the assumption that $\eta = 0$ exactly for both leads to a disagreement between the actual relative intensities of the peaks due to the first and second neighbors and those calculated by formula (12) of the Appendix. For example, we would expect the amplitude of peak *C* to be about twice that of *B*, but, in fact, they are about equal. We therefore postulate that the first-neighbor interaction has a nonzero η , sufficiently large to reduce the amplitude of peak *C* but insufficient to produce a distorted line shape. The results shown in Fig. 12 suggest a value of $\delta \approx 2.5$ corresponding to $\eta \approx 0.07$. Although no significant increase in the width of peak *C* due to nonzero η was observed, the

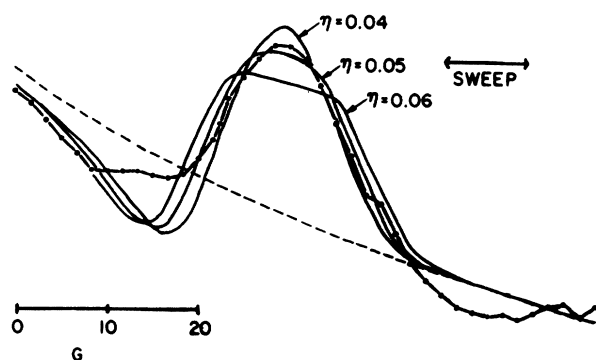


FIG. 7. The outer satellite (peak *E*) from the 155 kHz quadrupole interaction in the Al-0.4-at.-%-Mg alloy. dash-dot line: average of three experimental curves at 4.2°K; dashed line: assumed baseline; solid line: line shapes assuming different values of η , calculated by the theory described in the Appendix.

corresponding outer satellite *E* shown in Fig. 7 was significantly broadened. An attempt was made to estimate η by comparing this curve with theoretical shapes calculated for various values of this quantity. It will be seen from the figure that the best fit occurs for η between 0.04 and 0.06. Certainly a value higher than 0.06 seems unacceptable. A good experimental line shape was difficult to obtain because of the poor signal strength and sloping background, but it must be admitted that the fit of the line shape is not really satisfactory (considering the excellent fits obtained for the Al-Ga and Al-Ge alloys). It is possible that some other factor such as pairing of magnesium atoms is involved. Another indication of the nonideal nature of the alloy is the unusually large ratio of predicted to experimen-

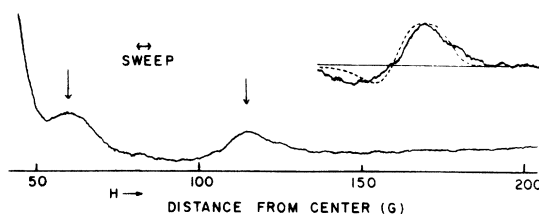


FIG. 8. ^{27}Al resonance curve from the Al-0.2-at.-%-Cu alloy, signal averaged over 190 5-min sweeps at 4.2°K. In the inset, the outer satellite peak is shown enlarged with a curve calculated assuming $\eta = 0.065$.

tal intensities of the satellite peaks listed in Table V. The average ratio is about 2.5, which indicates that only about 40% of the magnesium atoms are in truly random solid solution.

E. Aluminum-Copper

Quadrupole satellites from this alloy are shown in Fig. 8. Peaks at 58 ± 2 and 112 ± 2 G from the center may be associated with a quadrupole interaction $\nu_Q = 121 \pm 2$, presumably from the first neighbors. Although further structure due to nonaxial symmetry cannot be seen, the width of the peaks suggests that η is not exactly zero. A comparison of the outer peak with a theoretical shape with $\eta = 0.065$ is shown. (The usual value of σ , 4.7 kHz, has been assumed.) Although this must be considered the best estimate of η , it is clear that the fit of the curves is not satisfactory. The experimental curves have distinctly more tail than would be expected from a well-defined quadrupole interaction broadened by the usual Gaussian function. This could possibly be explained by the presence of two

TABLE V. Satellite peaks from the Al-0.4-at.-%-Mg alloy. Theoretical values were calculated with the parameters $N = 130$ and $\sigma = 4.7$ kHz: $\nu_Q = 155$ kHz and $\eta = 0.05$ for first-neighbor position (peaks *C*, *E*, and *F*), and $\nu_Q = 49$ kHz and $\eta = 0$ for the second-neighbor position (peaks *A*, *B*, and *D*).

Peak	Separation from center of resonance (G)	Amplitude relative to main resonance ($\times 10^{-5}$)	Type of singularity ^a	Satellite no. <i>n</i>	Theoretical separation (G)	Theoretical relative amplitude ($\times 10^{-5}$)
A	24.5 ± 1.0	50 ± 20	R	1	24.3	92
B	45.7 ± 1.0	19 ± 4	$\left\{ \begin{array}{l} R \\ S \end{array} \right.$	$\left. \begin{array}{l} 2 \\ 1 \end{array} \right\}$	46.2	$\left\{ \begin{array}{l} 40 \\ 12 \end{array} \right\}$ 48
C	72.0 ± 0.5	17 ± 3	X	1	72.0	77
D	91 ± 3	4 ± 2	S	2	88.2	4
E	140 ± 2	7 ± 2	$\left\{ \begin{array}{l} X \\ S \end{array} \right.$	$\left. \begin{array}{l} 2 \\ 1 \end{array} \right\}$	141	$\left\{ \begin{array}{l} 23 \\ 7 \end{array} \right\}$ 27
F	288 ± 10	2 ± 2	S	2	279	2

^aR is the inverse square-root infinity, S is the step singularity, and X is the unresolved step singularity and logarithmic infinity (discussed in the Appendix).

or more slightly different quadrupole interactions that could occur, for example, around a pair of copper atoms in adjacent positions. We would have to suppose that an appreciable fraction of the copper atoms were present in pairs, many more than would be expected in a random solution. The results of Minier¹⁵ also suggest that an appreciable agglomeration of copper atoms occurs in this system.

The experimental values of the amplitudes of the inner and outer satellite peaks relative to the main resonance were $(30 \pm 10) \times 10^{-5}$ and $(14 \pm 2) \times 10^{-5}$, respectively. These agree well with the theoretical values 46×10^{-5} and 16×10^{-5} , assuming $\nu_Q = 121$ kHz, $\eta = 0.065$, and $\sigma = 4.7$ kHz. The wipeout number N was taken to be¹⁰ 236 but for an alloy as dilute as this one the calculation is not sensitive to this consideration. It should be remarked that because of the possibility of preferred orientation in this rolled-foil sample, a disagreement between measured and calculated amplitudes would not have been surprising.

No peaks have been observed in addition to those noted above, and it is concluded that for the second neighbors $\nu_Q < 70$ kHz.

IV. SOLUTE RESONANCES

In two of the alloys, Al-Ga and Al-Cu, resonances of solute nuclei were observed. The Knight shift of the ⁶⁹Ga and ⁷¹Ga resonances were measured relative to a solution of GaCl₃ using the ²⁷Al resonance as an intermediate standard. Within experimental error, the shift of ⁶⁹Ga was the same at 4.2, 77, and 300 °K and had the mean value of $0.490 \pm 0.005\%$. The same value was obtained for the ⁷¹Ga resonance, which was measured at 300 °K only.

In the copper alloy, the following values were obtained for the frequency ratios of the aluminum and copper resonances at 4.2 °K in a field of ~ 14 kG:

$$\nu(^{63}\text{Cu})/\nu(^{27}\text{Al}) = 1.01914 \pm 0.00005,$$

$$\nu(^{65}\text{Cu})/\nu(^{27}\text{Al}) = 1.09171 \pm 0.00005.$$

Using the known Knight shift of aluminum (0.163% at 20 °K¹⁶) and the ratios of magnetic resonance frequencies of ²⁷Al, ⁶³Cu, and ⁶⁵Cu in the reference compounds AlCl₃ and CuCl₂,¹⁷ we deduce the Knight

shift of the copper nuclei in the alloy to be $0.35 \pm 0.01\%$. The values for both isotopes are the same within experimental error.

A trace of the ⁶³Cu resonance is shown in Fig. 9. The line is Gaussian except for slight extra tails that are probably due to quadrupole effects. The peak-to-peak derivative width is 5.4 ± 0.1 G. The same value was obtained for the ⁶⁹Ga resonance from the Al-Ga alloy (foil sample) at 4.2 °K. Here the fit to a Gaussian shape was within experimental error at all points. These curves were taken with a 40-Hz of modulation of peak-to-peak amplitude of 2.6 G. Making a small correction for this and neglecting the slight discrepancy in the tails of the ⁶³Cu curve, the mean-square width of both solute resonances is found to be 6.8 ± 0.4 G². The dipolar broadening calculated from Van Vleck's formula^{1,18} is 3.6 G². For this purpose, it is justifiable to assume that all neighbors of the solute atoms are ²⁷Al.

Thus a difference of about 3 G² remains to be explained. A similar discrepancy exists between the calculated and measured second moment of the ²⁷Al resonance in pure aluminum¹⁶ and has not been satisfactorily explained. Some of the extra broadening of the solute resonances might be attributed to indirect exchange (Rudermann-Kittel) interaction. If we make the rather improbable assumption that this interaction is as high as in copper,¹⁹ a contribution of ~ 1.5 G² to the second moment would be expected.

The amplitudes of the solute resonances were measured relative to those of the main ²⁷Al resonances in the same alloy. The comparisons were made at constant frequency, and the magnetic field was changed to bring in the desired resonances. No other changes were made to the spectrometer settings except the calibrated sensitivity control. The relative amplitude of the ⁶⁹Ga resonance (powder sample) was $(1.0 \pm 0.1) \times 10^{-3}$ and of the ⁶³Cu resonance, $(4.0 \pm 0.5) \times 10^{-4}$. By means of the wipeout numbers, we may relate the ²⁷Al resonance amplitude in the alloy to that in pure annealed aluminum in which the full resonance intensity is known to be observed. We can then use nuclear moments, spins, and isotopic abundances to obtain the theoretical relative intensities of the solute resonances, under the assumption that all the resonance transitions from all the solute nuclei of the given isotope contribute. These calculations were, of course, made in terms of integrated resonance intensities. To obtain results in terms of peak-to-peak amplitudes, conversion factors were required. These were obtained for each resonance involved by careful integration of good quality experimental resonance curves. In this way, we calculate that the ⁶⁹Ga and ⁶³Cu resonances have 0.30 ± 0.05 and 0.36 ± 0.05 of the possible intensities, respectively.

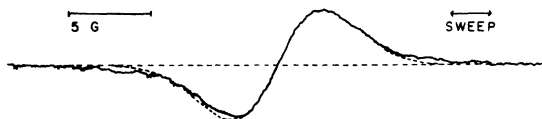


FIG. 9. Derivative magnetic resonance curve of ⁶³Cu in the Al-0.2-at.-%-Cu alloy at 4.2 °K, signal averaged over 190 5-min sweeps. The best-fitting Gaussian derivative curve is indicated by a dashed line.

Both these nuclei have $\frac{3}{2}$ spin, and thus 0.4 of the intensity arises from the transition $m = -\frac{1}{2}$ to $m = +\frac{1}{2}$ (the central transition). It is therefore concluded that the observed resonances are basically due to this transition only. The satellite transitions are completely wiped out by quadrupole interaction even for these small solute concentrations. This behavior is similar to that of the well-known ^{63}Cu resonance in copper-based alloys.^{1,20}

V. DISCUSSION OF QUADRUPOLE RESULTS

A summary of the quadrupole coupling parameters reported in this paper is given in Table III. Also included are results for dilute Al-Zn alloys determined by the same method and reported in a previous paper.¹¹

The results for the quadrupole interaction at the first neighbors of gallium, germanium, and magnesium agree within experimental error with those of Jørgensen, Nevald, and Williams⁶ using the single-crystal technique. The results of Minier²¹ obtained by the double-resonance field-cycling technique also agree for these alloys provided his assignment of quadrupole interactions to the different neighbor shells is revised. Since the largest quadrupole interactions in Al-Ga and Al-Ge were found to be axially symmetric within experimental error, Minier proposed that the interactions be assigned to the second- rather than the first-neighbor positions. But it is clear from the measurements reported in the present paper that Minier's proposal is not correct. The quadrupole interaction in Al-Ge is definitely nonsymmetric, and, although no asymmetry could be detected in the Ga alloy, intensity measurements do not allow the assignment of the 174-kHz interaction to the nearest-neighbor position. The nearly axial symmetry of these interactions must be accidental. The results for the silver alloy are also close to those found by Minier.²¹ The agreement on η is much better than for the Al-Zn system.

It was hoped that the quadrupole results would indicate some correlation with other alloy properties particularly with the valency and size of the solute atoms. In Table III data for a number of properties are included for comparison. The quadrupole interactions are, however, remarkably erratic, and no general conclusions can be drawn. Nevertheless, the following regularities can be noted: (a) In progressing along the series of increasing atomic number, copper, zinc, gallium, and germanium, a monotonic increase is observed in the quadrupole interaction at the nearest-neighbor position. (b) The interactions at the second-neighbor positions are correlated with the wipeout numbers, as far as the measurements go. (c) High values of η seem to be associated with small size differences between the solute and solvent atoms.

TABLE VI. Electric field gradients at aluminum nuclei at positions that neighbor solute atoms in aluminum.

Solute	Neighbor position	Electric field gradient, eq ($\text{esu} \times 10^{13}$)		
		Experiment	Theory ^a	
			A	B
Cu	1	9.5	-6.6	+0.9
	2	<4.3	+2.1	+3.0
Ag	1	10.4	-5.8	+2.0
	2	<5.0	+2.5	+3.4
Mg	1	9.5	-5.6	-2.4
	2	3.0	+1.0	+1.4
Zn	1	8.5	-4.5	-1.1
	2	1.5	+0.7	+1.1
Ga	1	10.7	+3.8	+4.6
	2	2.5	-0.1	-0.1
Ge	1	15.3	+9.4	+7.1
	2	<2.5	-0.6	-1.0

^aTheory of Fukai and Watanabe (Ref. 10) based on the dielectric function *A* without and *B* with exchange correction.

VI. COMPARISON OF RESULTS WITH THEORY

The most detailed theoretical treatment of the screening charge oscillations and the resultant field gradients around impurity atoms in aluminum has been given by Fukai and Watanabe.¹⁰ They used a pseudopotential theory that gave a good account of the residual resistivities of the dilute alloys.²²

The electric field gradients they obtained are compared with the experimental values in Table VI. The quadrupole moment Q of ^{27}Al has been assumed to be $0.15 \times 10^{-24} \text{ cm}^2$. Two sets of theoretical values exist that are based on different assumptions.

Although the agreement between theory and experiment is by no means satisfactory, the order of magnitude is correct, and the general trends of variation from alloy to alloy are reproduced. However, the theoretical values are generally too low by a factor of about 2. The signs of the field gradients cannot be checked because they cannot be determined from the experiments.

The variation of the field gradient with temperature is also of interest. It will be seen from Table IV that the temperature dependence of the quadrupole interaction is too large to be accounted for simply by the increase in internuclear distances due to lattice expansion. The increase in lattice constant is only 0.44% between 0 and 300 °K,²³ so that only about 1.5% variation in quadrupole interaction can be attributed directly to this. It is postulated, therefore, that the effect is due to the averaging of the quadrupole interaction over thermal oscillations of the aluminum atoms.

It is a reasonable simplification of the theory to suppose that the field gradient varies sinusoidally with distance from the solute atom over short intervals of distance. It may then be shown that, to a first approximation, the change $\Delta\nu_Q$ in the quadrupole interaction ν_Q , due to averaging over thermal oscillations of mean-square amplitude $\langle\chi^2\rangle$, is given by

$$\Delta\nu_Q/\nu_Q = -2\pi^2\langle\chi^2\rangle/\lambda.$$

The wavelength of the oscillations λ ($=\pi/k_f$, where k_f is the conduction-electron wave number at the Fermi surface³) is 1.5 Å for aluminum. Thus, taking $\langle\chi^2\rangle=0.01$ Å² at 300 °K,²⁴ we find $\Delta\nu_Q/\nu_Q = -0.06$, which provides a reasonable explanation of the temperature variation listed in Table IV.

VII. ASYMMETRY FACTOR AND SIZE EFFECT

A feature of the results not obtained from present theory is the asymmetry of the quadrupole interaction at the first-neighbor position. These results pose a difficult problem of interpretation. To explain the results in terms of conduction-electron screening effects, it is necessary to consider a nonspherically symmetric charge distribution around the solute atoms.

In the discussion of the results for Al-Zn,¹¹ it was noted that a reasonable explanation of the asymmetry factor could be obtained by approximating the screening charge distribution from charges centered on neighboring sites. Values as high as that observed, $\eta=0.25$, could be obtained if the charges on nearest-neighbor sites were opposite those on the solute atom. This would normally be expected from the charge-density oscillations. It was therefore anticipated that asymmetries of this order would be usual at the first-neighbor positions around solute atoms in dilute alloys. The additional results presented here show, however, that this is not the case. For the majority of alloys, η at the nearest-neighbor site is quite small.

A factor that may be important to the asymmetry problem is the distortion of the lattice due to the size difference between the solute and solvent atoms. In many cases, an appreciable change is observed in the lattice spacing on alloying (Table III).

An electrostatic calculation based on the movement of ions toward or away from the impurity center gives, at the nearest-neighbor position, a field gradient whose major principal axis is at right angles to that of the field gradient produced by the electronic charge distribution. Consequently, we expect to find large asymmetry factors when field gradients from these two sources are present. This might be expected when the size difference between the solute and solvent atoms is large. It will be seen from the results, however, that this is not the case. High asymmetry is associated with a

small rather than a large size difference.

It is thus concluded that there is no evidence that the size difference is an important factor in the determination of the quadrupole interaction or its asymmetry unless by a mechanism different from the one discussed here.

VIII. CONCLUSION

Quadrupole interactions at sites that neighbor solute atoms have been measured in a number of dilute aluminum alloys by conventional NMR using polycrystalline samples. The sensitivity compares favorably with the single-crystal method, and sample preparation is easier but, of course, no information about the orientation of the principal axes can be obtained. In Al-Ga and Al-Ge, sufficient sensitivity was available to enable measurements to be made at room temperature.

The technique is certainly less sensitive than the field-cycling method used by Minier²¹ but has the advantage of simple interpretation of measured signal intensities. This is helpful in assigning quadrupole interactions to the different neighbor positions.

Although the magnitudes of the quadrupole interactions found are in general agreement with the theories of Blandin and Friedel³ and Fukai and Watanabe,¹⁰ completely satisfactory understanding of the results is lacking and must await further development of theory. There seems to be no doubt of the existence of oscillations of conduction-electron density around the solute atoms. The temperature dependence of the quadrupole interactions may be explained in these terms. The size difference between the solute and solvent atoms does not appear to play an important part in determining quadrupole interactions.

The Knight shifts of the solute nuclei ⁶⁹Ga and ⁶³Cu have also been measured. It has been shown that these resonances are affected by quadrupole interactions because the observed intensities correspond to the central $-\frac{1}{2}$ to $+\frac{1}{2}$ transitions only. The mean-square width of these resonances was greater than could be explained by dipolar broadening alone.

ACKNOWLEDGMENTS

The author wishes to thank Dr. N. L. Peterson, Dr. J. B. Darby, Jr., and Dr. F. Y. Fradin for their support of the work and J. W. Downey, L. C. Robinson, and F. J. Karasek for assistance in sample preparation, and Dr. T. J. Rowland and Dr. M. Minier for the loan of samples.

APPENDIX: FIRST-ORDER QUADRUPOLE PERTURBATION IN POLYCRYSTALLINE SAMPLE

A. Basic Powder Pattern

For a given quadrupole interaction in a given crystallite, the frequency of the satellite transition

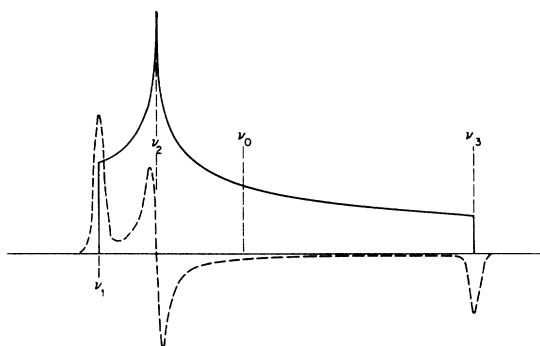


FIG. 10. NMR first-order-perturbation powder pattern for a satellite transition that results from a nonaxially symmetric quadrupole interaction. The unperturbed resonance position is ν_0 , and the singularities at ν_1 , ν_2 , and ν_3 are shown. The dashed curve is an illustration of a broadened derivative resonance curve.

between the $(n - \frac{1}{2})$ and $(n + \frac{1}{2})$ magnetic quantum levels is given by²⁵

$$\nu = \nu_0 + \frac{1}{2} n \nu_Q (3 \cos^2 \theta - 1 + \eta \sin^2 \theta \cos 2\phi), \quad (1)$$

where θ and ϕ are the spherical polar coordinates of the magnetic-field direction with respect to the principal axes of the quadrupole interaction. The parameter ν_Q is related to the quadrupole coupling constant $e^2 q Q / h$ as follows:

$$\nu_Q = \frac{3}{2I(2I-1)} \frac{e^2 q Q}{h}. \quad (2)$$

Assuming that all orientations of the crystallites are equally probable, the normalized line-shape function may be shown to be²⁵

$$f_n(\nu) = \frac{1}{n \nu_Q} P_n \left(\frac{\nu - \nu_0}{n \nu_Q} \right), \quad (3)$$

where

$$P_n(x) = (1/\pi a) K [\sin^{-1}(b/a)] \quad \text{if } -\frac{1}{2}(1+\eta) < x < -\frac{1}{2}(1-\eta),$$

$$P_n(x) = (1/\pi b) K [\sin^{-1}(a/b)] \quad \text{if } -\frac{1}{2}(1-\eta) < x < 1,$$

$$P_n(x) = 0 \quad \text{otherwise,}$$

$$a = [\eta(1-x)]^{1/2},$$

and

$$2b = [(3-\eta)(1+\eta+2x)]^{1/2}.$$

K denotes the complete elliptic function of the first kind. Steps in the function occur for $x = -\frac{1}{2}(1+\eta)$ and $x = 1$ and at $x = -\frac{1}{2}(1-\eta)$ there is an infinity. These singularities are the only easily recognizable features of the powder pattern, particularly where the derivative resonance curve is observed with the af modulation method of detection. An example of a powder pattern and broadened derivative curve is shown in Fig. 10.

B. Calculation of Amplitudes of Peaks That Arise From Singularities

Substitution of the values of x at the singularities in Eq. (3) shows that the amplitudes of the steps in $f_n(\nu)$ are

$$\alpha_1 / n \nu_Q \quad \text{at } \nu_1 = \nu_0 - \frac{1}{2} n \nu_Q (1 + \eta),$$

$$\alpha_3 / n \nu_Q \quad \text{at } \nu_3 = \nu_0 + n \nu_Q,$$

and close to the infinity at $\nu_2 = \nu_0 - \frac{1}{2} n \nu_Q (1 - \eta)$ we may approximate as follows:

$$f_n(\nu) \approx \frac{\alpha_2}{\pi n \nu_Q} \left(\ln \Delta - \ln \left| \frac{\nu - \nu_2}{n \nu_Q} \right| \right) \quad (4)$$

where

$$\alpha_1 = [2\eta(3+\eta)]^{-1/2}, \quad \alpha_2 = [2\eta(3-\eta)]^{-1/2},$$

$$\alpha_3 = (9 - \eta^2)^{-1/2},$$

and

$$\Delta = 16\eta(3-\eta)/(3+\eta).$$

To obtain line shapes for comparison with experiment, we must include a broadening function $g(\nu)$ that is normally due to magnetic dipole interactions. This will be assumed to be Gaussian with the root-mean-square (rms) width σ as follows:

$$g(\nu) = (2\pi)^{-1/2} \sigma^{-1} e^{-\nu^2/2\sigma^2}. \quad (5)$$

Convolution of $g(\nu)$ with $f_n(\nu)$ followed by differentiation yields the line shapes near the singularities given by

$$h_1(\nu) = \frac{\alpha_1}{n \nu_Q} g(\nu - \nu_1),$$

$$h_2(\nu) = \frac{\alpha_2}{2^{1/2} \sigma \pi n \nu_Q} D \left(\frac{\nu - \nu_2}{2^{1/2} \sigma} \right), \quad (6)$$

$$h_3(\nu) = -\frac{\alpha_3}{n \nu_Q} g(\nu - \nu_3),$$

where

$$D(x) = \int_{-\infty}^{\infty} e^{-(x-t)^2} dt/t. \quad (7)$$

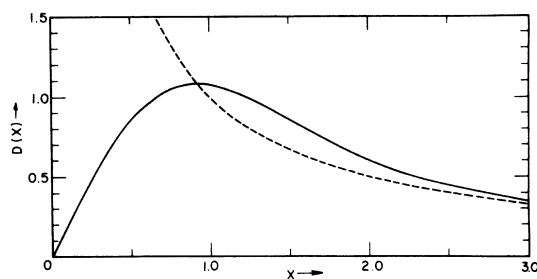


FIG. 11. Graph of the function $D(x)$ that results from the convolution of a Gaussian function with the derivative of a logarithmic infinity. The unbroadened derivative is shown by the dashed curve.

This function results from the convolution of a Gaussian function with the derivative of a logarithmic infinity. It may be written in the following form, which is more convenient for numerical evaluation:

$$D(x) = 2e^{-x^2} \int_0^x e^{t^2} dt. \quad (8)$$

The function is plotted in Fig. 11.

We may now deduce the following formula for amplitude A of the peaks at ν_1 , ν_2 , and ν_3 relative to the peak-to-peak derivative amplitude A_0 that the satellite would have in the absence of quadrupole interaction:

$$A/A_0 = \alpha\beta\sigma e^{1/2}/2n\nu_Q, \quad (9)$$

where $\alpha = \alpha_1, \alpha_2$, or α_3 . For a step singularity, A refers to the peak amplitude of the derivative curve, and $\beta = 1$. For a logarithmic infinity, A refers to the peak-to-peak amplitude, and $\beta = 1.221$.

For a solid solution of atomic concentration c that contains a quadrupole interaction ν_Q at each of Z crystallographically equivalent neighbors around a solute atom, we deduce

$$\frac{A}{A_0} = \frac{3Zc\alpha\beta e^{1/2} [(I + \frac{1}{2})^2 - n^2]}{4I(I+1)(2I+1)} \frac{\sigma}{n\nu_Q} K, \quad (10)$$

where A_0 is the peak-to-peak amplitude of the main resonance, and the probabilities of the satellite transitions are proportional to $[(I + \frac{1}{2})^2 - n^2]$.

The reduction factor K arises from quadrupole broadening produced by solute atoms other than those which actually give rise to the satellite peak (i. e., the correction is due to overlapping of quadrupole interactions). The assumption will be made that the "wipeout" approximation applies as found empirically for the main resonance. This may be justified on the basis of the additivity of quadrupole shifts in first-order perturbation, assuming random solid solution and that the width of the satellite peak is roughly the same as that of the central resonance. Thus the reduction of the satellite peaks is taken to be the same as that of the satellite component of the main resonance. A correction factor, however, is required in formula (10) because the main resonance also contains a central ($n=0$) component that is not affected by the quadrupole interactions. We thus deduce

$$K = \left(1 + \frac{3(2I+1)}{8I(I+1)} [(1-c)^{-N} - 1]\right)^{-1}. \quad (11)$$

Strictly, slightly different wipeout numbers should be used for the inner and outer satellites. Unfortunately, measurements on the main resonance yield only a mean value; consequently, this effect cannot be taken properly into account. It should be remembered, however, that the true K for the inner satellites may be slightly larger than given by formula (11) and K for the outer satellites

slightly less. Because of these uncertainties, this correction factor should be regarded as approximate only.

We now consider the special case of axial symmetry $\eta=0$. The treatment of the singularity at ν_3 is unchanged, but those at ν_1 and ν_2 become coincident and the singularity becomes an infinity of the inverse square-root type. The derivation of this line shape and its convolution with a Gaussian broadening function have been discussed elsewhere,²⁶ and the application of those results to the dilute alloy problem leads to the following formula for the ratio of peak-to-peak amplitudes of the satellite and main resonances:

$$\frac{A}{A_0} = 0.987Zc \left(\frac{\sigma}{n\nu_Q}\right)^{1/2} K \frac{[(I + \frac{1}{2})^2 - n^2]}{I(I+1)(2I+1)}. \quad (12)$$

C. Line-Shape Calculation For Near-Axial Symmetry

A situation commonly arising at the nearest-neighbor position in dilute alloys (with fcc structure) is that η is nonzero. However, η is not sufficiently large for the individual peaks corresponding to the singularities at ν_1 and ν_2 to be properly resolved. It is then necessary to estimate η from the recorded line shapes. To facilitate this, theoretical curves for these partially resolved situations were calculated assuming a Gaussian broadening function.

Provided we consider only the region close to the almost coincident singularities ν_1 and ν_2 , we may derive the following approximation from Eq. (3):

$$f_n(\nu) = \frac{1}{n\nu_Q(6\eta)^{1/2}} p\left(\frac{\nu - \nu_s}{\eta\nu_Q}\right), \quad (13)$$

where $\nu_s = -\frac{1}{2}n\nu_Q$ (i. e., the position of the singu-

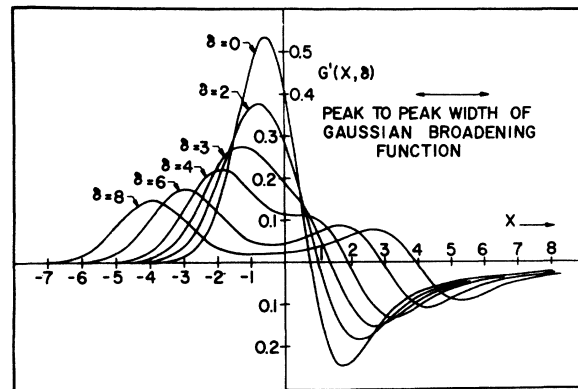


FIG. 12. Derivative line shapes of a satellite peak due to a slightly asymmetric quadrupole interaction in a polycrystalline sample. The curves were calculated for various values of the parameter δ , the ratio of the separation of the step and logarithmic singularities to the rms width of the Gaussian broadening function.

larity when $\eta = 0$, and the function $p(t)$ is given by

$$p(t) = (2/\pi) (t + \frac{1}{2})^{-1/2} K \{ \sin^{-1} [(t + \frac{1}{2})^{-1/2}] \} \text{ if } t > \frac{1}{2},$$

$$p(t) = (2/\pi) K \{ \sin^{-1} [(t + \frac{1}{2})^{1/2}] \} \text{ if } -\frac{1}{2} < t < \frac{1}{2}$$

$$p(t) = 0 \text{ if } t < -\frac{1}{2}.$$

Convolution with the Gaussian broadening function $g(\nu)$ and differentiation yield the following line shape:

$$h_{12}(\nu) = (6n\nu_0\sigma^3)^{-1/2} G[(\nu - \nu_s)/\sigma, \delta], \quad (14)$$

where

$$G'(x, \delta) = \frac{1}{(2\pi\delta)^{1/2}} \int_{-\infty}^{\infty} (y-x) e^{-(x-y)^2/2} p\left(\frac{y}{\delta}\right) dy. \quad (15)$$

The line shape thus depends on the one parameter $\delta = n\eta\nu_0/\sigma$, i. e., the ratio of the separation of the singularities ν_1 and ν_2 to the rms width of the broadening function.

Curves were calculated as required for compari-

son with experiment, and the results for a number of values of δ are shown in Fig. 12. Also included is the curve for $\delta = 0$ on the same scale, taken from a calculation in a previous paper.²⁶ The derivative function $G'(x)$ that appears in the Appendix of that paper is the same as $G'(x, 0)$ in the present notation.

Reference to the axially symmetric case is often convenient as the signal amplitude for that case may be readily calculated from formula (12).

It will be seen from the figure that there is a significant reduction in signal amplitude for δ greater than about 2. The change in line shape becomes obvious for $\delta > 3$, but actual resolution of two independent peaks requires $\delta > 5$. In applying these results to the analysis of line shapes for an even value of n and half-integral I (e. g., the outer satellites of ²⁷Al), it must be remembered that a small peak from the ν_3 step singularity of the $-\frac{1}{2}n$ satellite will be superimposed on the pattern. This reduces the resolution obtainable.

*Work performed under the auspices of the U.S. Atomic Energy Commission.

†Present address: Materials Physics Div., Atomic Energy Research Establishment, Harwell, Didcot, Berks, England.

¹N. Bloembergen and T. J. Rowland, *Acta Metall.* **1**, 731 (1953).

²T. J. Rowland, *Acta Metall.* **3**, 74 (1955).

³A. Blandin and J. Friedel, *J. Phys. Radium* **21**, 689 (1960).

⁴W. Kohn and S. H. Vosko, *Phys. Rev.* **119**, 912 (1960).

⁵R. T. Schumacher and G. Schnackenberg, *Solid State Commun.* **7**, 1735 (1969).

⁶L. Jorgensen, R. Nevald, and D. Ll. Williams, *J. Phys. F* **1**, 972 (1971).

⁷L. E. Drain, *Rev. Sci. Instrum.* **43**, 1648 (1972).

⁸Department of Mining, Metallurgy, and Petroleum Engineering, University of Illinois, Urbana, Ill.

⁹Laboratoire de Spectrometrie Physique, Universite Scientifique et Medicale de Grenoble, France.

¹⁰Y. Fukai and K. Watanabe, *Phys. Rev. B* **2**, 2353 (1970).

¹¹L. E. Drain, *J. Phys. C* **1**, 1690 (1968).

¹²H. Zoller, *Metall* **11**, 378 (1957).

¹³C. Berthier and M. Minier, *Solid State Commun.* **10**, 257 (1972).

¹⁴N. Fernelius and C. P. Slichter, *Proc. Colloq. AMPERE* **15**, 347 (1969).

¹⁵M. Minier, Ph.D. thesis (University of Grenoble, 1968) (unpublished).

¹⁶L. E. Drain, *Metall. Rev.* **12**, 195 (1967).

¹⁷H. E. Walchli, ORNL Report No. 1775, 1954 (unpublished).

¹⁸J. H. Van Vleck, *Phys. Rev.* **74**, 1168 (1948).

¹⁹E. R. Andrews, J. L. Carolan, and P. J. Randall, *Phys. Lett. A* **37**, 125 (1971).

²⁰T. J. Rowland, *Phys. Rev.* **119**, 900 (1960).

²¹M. Minier, *Phys. Rev.* **182**, 437 (1969).

²²Y. Fukai, *Phys. Rev.* **186**, 697 (1969).

²³W. B. Pearson, *A Handbook of Lattice Spacings and Structures of Metals and Alloys* (Pergamon, New York, 1958), p. 313.

²⁴*International Tables for X-ray Crystallography* (Kynoch, Birmingham, England, 1962), Vol. 3, p. 237.

²⁵M. H. Cohen and F. Reif, *Solid State Phys.* **5**, 321 (1957).

²⁶L. E. Drain, *Proc. Phys. Soc. Lond.* **88**, 111 (1966).